

# Study on preparation technology of $^{64}\text{Cu}$ radionuclide target

Haitao Bai<sup>1,†</sup>, Chao Pan<sup>1</sup>, Furong Li<sup>1</sup>, Yang Du<sup>1</sup>, Yifei Cao<sup>1</sup>, Feihu Yang<sup>1</sup>, Tao Zhang<sup>1</sup>,

(1. Sichuan Sichuan Longevous BeamTech Co., LTD., Mianyang 621900, China)

**Abstract:** **Purpose:** The target preparation technology of  $^{64}\text{Cu}$  radionuclides, the quality control scheme of isotope target thickness and the yield of  $^{64}\text{Cu}$  radionuclides were systematically studied. **Methods:** 1. Based on the nuclear reaction principle of beam interaction with matter, the nuclear reaction cross section ratio parameter and the nuclear reaction probability ratio parameter were proposed to evaluate the target thickness and isotope yield. 2. A detailed solid target irradiation design was put forward, the Bethe-Block formula was used to derive the calculation method of target thickness in detail, and the mass thickness of the target (mass surface density) was used to control the thickness of the target. 3. According to Faraday's first and second electrolytic laws, the electroplating device model was designed and the electroplating process was proposed. **Results:** 1. SRIM software was used to calculate the stopping power of different density targets in detail, and the energy was matched according to the theoretical formula 2. The nuclear reaction cross section ratio and the nuclear reaction probability ratio were calculated of 10.5MeV proton incident on  $^{64}\text{Ni}$  target and exiting target with different energies. The results of the two parameters are similar, however the nuclear reaction probability ratio is added with the stopping power parameter, the nuclear reaction probability ratio parameter is larger and has more evaluation significance. 3. SRIM software was used to calculate the thickness and mass thickness parameters of the proton exiting target with different densities and different energies. The results showed that the yield efficiency is 91.94% and the required target cost is only 66.39% when the proton exiting target energy is 5.5MeV versus 0MeV. 4. The electrochemical equivalent of Ni and electroplating time parameters were calculated according to Faraday's electrolysis law, and  $^{64}\text{Ni}$  target was electroplated on the gold target holder. The electroplated target was irradiated with 11MeV proton beam, 48.97 $\mu\text{A}$ , for 6 hours, and the radiation activity of  $^{64}\text{Cu}$  was 1.34Ci, and its half-life was consistent with the expected results. **Conclusion:** The target preparation technology and electroplating theory of  $^{64}\text{Cu}$  radionuclides were systematically studied. For expensive isotope targets, the nuclear reaction cross-section ratio and the nuclear reaction probability ratio were proposed to evaluate the thickness of the target. By this method, the isotope targets can be greatly saved without seriously affecting the yield. This paper has theoretical and practical guiding significance for the design and preparation of isotope targets.

<sup>†</sup>Corresponding author, Haitao Bai, Ph.D., Cyclotron target design, [binary113@163.com](mailto:binary113@163.com)

**Key words:**  $^{64}\text{Ni}$  target design;  $^{64}\text{Cu}$  radionuclides; Isotope yield; Target plating

The half-life of  $^{64}\text{Cu}$  is 12.7h, and the main decay modes are  $\beta^+$  (0.65308MeV, 17.4%),  $\beta^-$  (0.5789MeV, 39%), EC (43%), so  $^{64}\text{Cu}$  can be used as a PET/CT diagnostic nuclide, and also can be used as a cancer treatment nuclide<sup>[1][2][3]</sup>. The role of copper in human cancer cell metabolism has been extensively studied over the past 20 years, and a close relationship between copper and cancer progression has been demonstrated. In 2013, Laura Evangelista and other Italian scholars discussed the difference between the content of copper in cancer cells and normal cells, and the involvement of copper in tumor angiogenesis and non-neoplastic diseases such as neurodegenerative diseases<sup>[4]</sup>. In 2016, Paola Panichelli et al. in Italy applied  $^{64}\text{CuCl}_2$  to the diagnosis of brain astroglioma, and diagnosed 19 patients, and the PET/CT and MRI results were in good agreement<sup>[5]</sup>. In 2020, Kristoffer Kjærgaard et al in Denmark studied the hepatic removal kinetics, biological distribution and radiation dosimetry of  $^{64}\text{Cu}$  in 6 healthy patients respectively through intravenous and oral input. It was found that both intravenous and oral doses of 50MBq of  $^{64}\text{Cu}$  were sufficient for continuous PET/CT studies in humans<sup>[6]</sup>. In 2022, Gabriela Capriotti et al. from Italy clarified that copper ions play an important role in many biological processes, copper is a cofactor of many enzymatic reactions, a structural component of different proteins, and a key regulator of cell proliferation and growth, and copper is highly accumulated in a variety of tumors in its simple ionic form.  $^{64}\text{CuCl}_2$  has been successfully applied in PET imaging of prostate cancer, bladder cancer, glioblastoma multiforme, and non-small cell lung cancer, and  $^{64}\text{CuCl}_2$  is expected to be used as a therapeutic nuclide<sup>[7]</sup>.

In addition, drug labeling of  $^{64}\text{Cu}$  has also entered the frontier of nuclear medicine. In 2019, Marc Pretze et al. in Germany conducted a  $^{64}\text{Cu}$ -Nodaga-aunps labeling study on  $^{64}\text{Cu}$ <sup>[8]</sup>. In 2020, Garima Singh et al. reported the synthesis of novel BFCs based on the hexadendate bis(amine)tetrakis(pyridine) bispidine-9-ol<sup>[9]</sup>. In 2021, James H. McMahon et al. conducted a clinical study on non-invasive imaging of HIV infected people and uninfected controls using anti-HIV antibodies labeled  $^{64}\text{Cu}$ <sup>[10]</sup>. In 2022, Daniel F. Earley et al. successfully demonstrated the feasibility of photochemically induced conjugacy methods for the development of copper-based radiotracers for diagnostic positron emission tomography (PET) imaging and targeted radionuclide therapy<sup>[11]</sup>. In 2023, Olga O. Krasnovskaya et al. in Russia systematically studied the labeling drugs of copper. It mainly includes  $[^{64}\text{Cu}]\text{Cu-DOTA-TOC}$ 、 $[^{64}\text{Cu}]\text{Cu-DOTA-TATE}$ 、 $[^{64}\text{Cu}]\text{Cu-PSMA-ALB-89}$ 、 $[^{64}\text{Cu}]\text{Cu-PSMA-ALB-89}$ 、 $[^{64}\text{Cu}]\text{Cu-RSP-085}$ 、 $[^{64}\text{Cu}]\text{Cu-RSP-085}$  etc.<sup>[12]</sup>.

At present, the main nuclear reaction principles of  $^{64}\text{Cu}$  production are:  $^{64}\text{Ni}(\text{p},\text{n})^{64}\text{Cu}$ 、 $^{64}\text{Ni}(\text{d},2\text{n})^{64}\text{Cu}$ , thermal neutron capture  $^{63}\text{Cu}(\text{n},\gamma)^{64}\text{Cu}$ , fast neutron reaction  $^{64}\text{Zn}(\text{n},\text{p})^{64}\text{Cu}$ . In order to meet the needs of  $^{64}\text{Cu}$  scientific research and clinical application, it is necessary to solve the corresponding  $^{64}\text{Ni}$  target supply problems, accelerator target design problems,  $^{64}\text{Cu}$  nuclide separation and purification problems, and put forward strict quality control standards in all aspects, only in this way can ensure the stable supply of  $^{64}\text{Cu}$ . In 1991, Guoji Xu et al. proposed a nuclear target thickness uniformity measurement scheme, including balance weighing method (direct, destroyed, twice), quartz crystal measurement, equivalent air alpha particle measurement, ion beam backscattering method, optical absorption method, etc. [13]. In 1995, Guoji Xu continued to put forward research on isotope target preparation technologies, including vacuum evaporation, focused heavy ion beam sputtering, rolling, electroplating, centrifugal precipitation, etc. [14]. In 1997, Deborah W. McCarthy et al. used the CS-15 cyclotron to produce 15.5MeV and 11.4MeV protons. The  $^{64}\text{Ni}$  target was irradiated and  $^{64}\text{Cu}$  of about 600mCi was obtained with a yield of 5.0mCi/( $\mu\text{Ah}$ ) [15]. In 2003, Atsushi Obata et al. used a 12MeV proton cyclotron to conduct  $^{64}\text{Cu}$  targeting research, and obtained an average yield of  $^{64}\text{Cu}$  of 1.983 mCi/( $\mu\text{Ah}$ ) [16]. In 2009, Jung Young Kim et al in South Korea used a 50MeV cyclotron to study the preparation of the target, and actually produced a beam of 18MeV, 30~50 $\mu\text{A}$ , shooting the target for 1 hour, and obtained a yield of about 20mCi/h. The flow intensity was calculated as 40 $\mu\text{A}$ , and the yield was 0.5mCi /( $\mu\text{Ah}$ ) [17]. In 2016, Xilin Sun et al. used cyclotron to produce 16.5MeV protons to carry out research on target preparation, electroplating, purification and other work [18]. In 2017, Qinghua Xie et al. used the accelerator to generate 20MeV protons and obtained  $^{64}\text{Cu}$  of about 200mCi through  $^{64}\text{Ni}(\text{p},\text{n})^{64}\text{Cu}$  reaction [19]. In 2021, Maite Jauregui-Osoro et al. in London, UK, used a cyclotron to generate 11MeV and 30 $\mu\text{A}$  protons to bombard a  $^{64}\text{Ni}$  target for 8 hours, obtaining  $^{64}\text{Cu}$  of 3.67GBq (99mCi), with a converted yield of 0.41 mCi/( $\mu\text{Ah}$ ) [20]. In 2023, Ivanna Hrynchak et al. from Portugal studied the  $^{64}\text{Cu}$  solution for solid target and liquid target, and obtained yields of 13.5GBq and 2.8GBq, respectively. According to the data in the paper, the converted yields were 2.4mCi/( $\mu\text{Ah}$ ) and 0.34mCi/( $\mu\text{Ah}$ ) respectively [21].

From the perspective of  $^{64}\text{Cu}$  target preparation scheme, the main problems currently exist are: (1) The tightness of the target obtained by different target preparation processes is different, some loose, some tight, and a unified method is needed to determine the thickness of the target. (2) It is difficult to find non-destructive testing methods in thickness testing: The EDXRF method is limited by the relationship between X-ray energy and thickness, and the alpha step meter test needs to destroy the sample. In this

paper, the preparation technology of radioisotope  $^{64}\text{Cu}$  target was studied based on the LB-11MTS proton cyclotron of Sichuan Longevous BeamTech Co., LTD. The accelerator mainly provides 11MeV proton beam with the target current intensity of about 100 $\mu\text{A}$ . The main research contents of this paper include: The influencing factors of plating thickness were systematically studied, the target plating equipment and plating thickness quality control scheme were proposed, and the influencing factors of  $^{64}\text{Cu}$  yield were calculated in detail. The nuclear reaction cross ratio and the reaction probability ratio are used to calculate the energy deposition on the target. A target electroplating device was proposed for the LB-11MTS proton cyclotron. And the electroplated target was tested for the production of  $^{64}\text{Cu}$ .

## 1 Materials and Methods

### 1.1 Calculation of the nuclear reaction cross section ratio and the nuclear reaction probability ratio

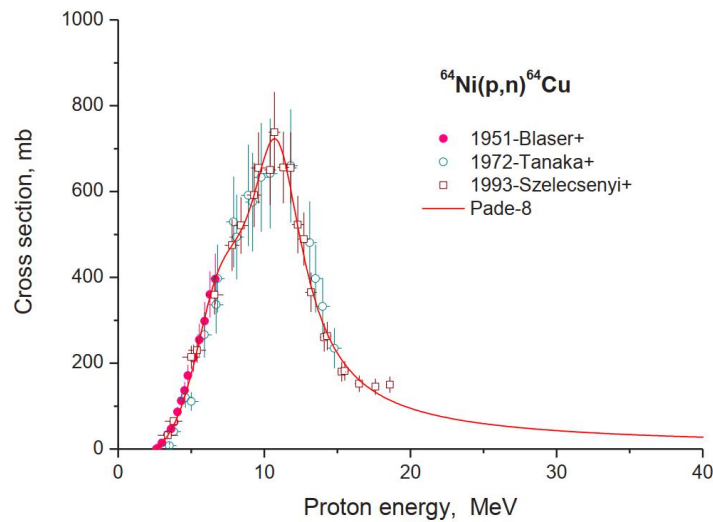


**Fig. 1** Nuclear reaction cross section of  $^{64}\text{Ni}(p,n)^{64}\text{Cu}$ <sup>[2][22]</sup>

The cross section of  $^{64}\text{Ni}(p,n)^{64}\text{Cu}$  nuclear reaction based on proton beam is shown in Fig. 1. The nuclear reaction threshold energy is 2.6MeV, the maximum cross section of the nuclear reaction is about 659.5mb when the proton beam energy is 11MeV, When the proton beam energy is 4MeV, 4.5MeV and 5MeV, the cross sections of the nuclear reaction are 82.4mb, 131.5mb and 193.6mb, respectively<sup>[23]</sup>. When the beam energy is low, the nuclear reaction cross section is much smaller than the maximum nuclear reaction cross section corresponding to the beam 11MeV. Therefore, to save  $^{64}\text{Ni}$  materials and reduce the thickness of the  $^{64}\text{Ni}$  target, the cutoff energy of the beam on the target can be considered as 4~5MeV. The

specific evaluation scheme is evaluated from the nuclear reaction cross section ratio and the nuclear reaction probability ratio. The specific evaluation process is shown in Fig. 2:

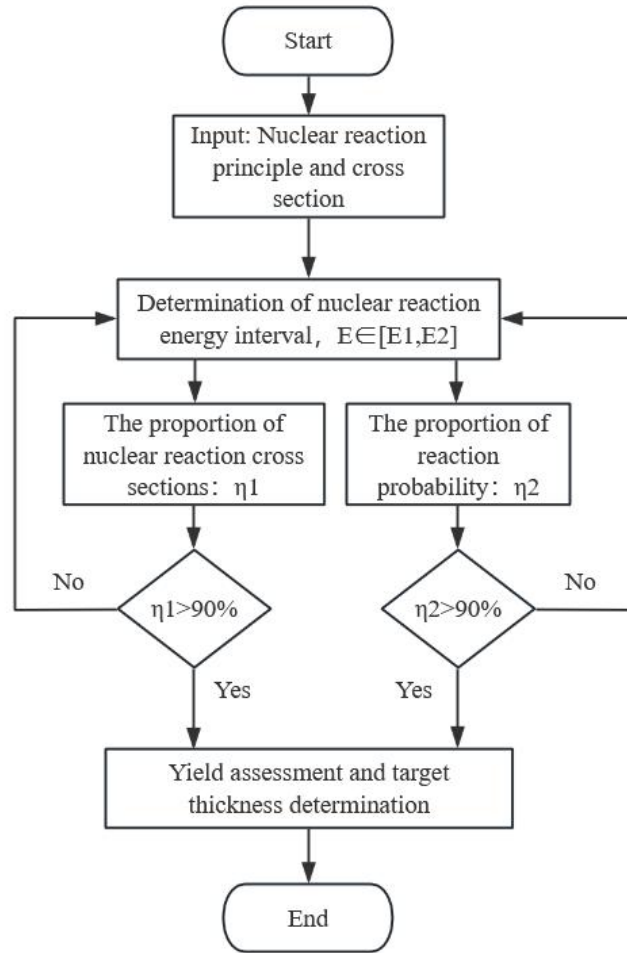


**Fig. 2 Assessment process of nuclear reaction cross section proportion and nuclear reaction probability proportion**

In Fig. 2, it is necessary to calculate the nuclear reaction cross section ratio and the nuclear reaction probability ratio. The specific calculation principle is based on the thick target nuclear reaction formula<sup>[24]</sup>:

$$P = N_v \int_0^D \sigma(E) \cdot dx = N_v \int_0^{R(E_0)} \sigma(E) \cdot dx \dots\dots\dots (1)$$

Where :  $N_v$  is the number of target nuclei per unit volume,

$$N_v = \frac{N}{V} = \frac{\frac{m_{TargetMaterial}}{M_A} \cdot N_A}{V} = \frac{\rho \cdot N_A}{M_A}, \rho \text{ is the density of the target, } M_A \text{ is the relative atomic}$$

mass,  $N_A$  is the Avogadro constant,  $E_0$  is the initial energy of the proton beam,  $D$  is the thickness of the target,  $\sigma(E)$  is the cross section of a beam with energy E to undergo a nuclear reaction in the target.

Transform the beam energy with the depth of the beam in the target:

$$P = N_v \int_{E_0}^0 \sigma(E) \frac{dE}{dE/dx} = N_v \int_0^{E_0} \left[ \frac{\sigma(E)}{-dE/dx} \right] \cdot dE \dots\dots\dots (2)$$

Where:  $-dE/dx$  is the stopping power of the target to the beam, which is related to the type of the target and the beam energy. The energy loss formula of interactions between heavy charged particles such as protons and alpha particles with matter is expressed as<sup>[24]</sup>:

$$-\frac{dE}{dx} = \frac{4\pi z^2 e^4 Z N_v}{mv^2} \left[ \ln\left(\frac{2mv^2}{I}\right) - \ln(1 - \beta^2) - \beta^2 \right] \dots\dots\dots (3)$$

By introducing formula (3) into formula (2), the yield of nuclide is not correlated with the atomic density  $N_v$ . Plug  $N_v = \frac{\rho \cdot N_A}{M_A}$  into the above equation to get:

$$-\frac{dE}{dx} = \frac{4\pi z^2 e^4 Z \cdot \rho \cdot N_A}{m \cdot (v^2 \cdot M_A)} \left[ \ln\left(\frac{2mv^2}{I}\right) - \ln(1 - \beta^2) - \beta^2 \right] \dots\dots\dots (4)$$

Therefore, the energy loss (or stopping power) generated by the interaction of heavy charged particles such as protons and alpha particles with matter is related to the atomic number  $Z$  of the target, the relative atomic mass  $M_A$ , the charge number  $z$  of the charged particle, and the density  $\rho$  of the target, and the stopping power  $-dE/dx$  is proportional to the density  $\rho$  of the target, and because of  $v^2 \cdot M_A = 2E$ , the stopping power is inversely proportional to the beam energy. In formula (4),  $m$  is the rest mass of the electron,  $v$  is the laboratory reference frame velocity of the beam particle,  $\beta = v/c$  is the relativistic velocity of the beam particle, and  $I \approx 9.1Z(1 + 1.9Z^{-2/3})$  is the average excited energy level of the atom when eV is the unit.

The formula of saturation yield and particle number of nuclear reaction  $I_M$  (Particles/s) are as follows:

$$Y_{sat} = P \cdot I_M \dots\dots\dots (5)$$

$$I_M = \frac{I_e}{N_e \cdot q_e} = \frac{I_e}{Z \cdot q_e} \dots\dots\dots (6)$$

Where  $N_e$  is the number of charged charge of the beam, that is, proton  $N_e = 1$  and alpha particle charge  $N_e = 2$ .  $q_e$  is the coulomb number corresponding to a single charge, namely:  $q_e = 1.602 \times 10^{-19} C$ . Thus, the yield at any time can be obtained as follows:

$$Y = Y_{sat} \cdot (1 - e^{-\lambda \cdot t}) \dots\dots\dots (7)$$

Where:  $\lambda = \frac{\ln 2}{T_{1/2}} = \frac{0.693}{T_{1/2}}$  is the nuclear reaction constant.

In Fig. 2,  $\eta_1$  is the cross-section proportion of the selected nuclear reaction energy interval ( $E \in [E_1, E_2]$ ) in the entire energy interval, and  $\eta_2$  is the corresponding probability proportion of nuclear reaction. The two formulas are as follows:

$$\eta_1 = \frac{\int_{E_1}^{E_2} \sigma(E) dE}{\int_0^{E_0} \sigma(E) dE} \dots\dots\dots (8)$$

$$\eta_2 = \frac{\int_{E_1}^{E_2} \frac{\sigma(E)}{-dE/dx} dE}{\int_0^{E_0} \frac{\sigma(E)}{-dE/dx} dE} \dots\dots\dots (9)$$

In the evaluation of formula (9), although the stopping power  $-dE/dx$  of the target for heavy charged particles is proportional to the density  $\rho$  of the target according to formula (4), and the density of the target prepared by actual electroplating is unknown, the upper and lower limits of the integral of the formula represent the sum of the integral of the stopping power  $-dE/dx$  during the interaction between the beam and the target. Therefore, the sum of beam energy attenuation is fixed according to formulas (1) and (2), so even if the density of the target is not clear, if the upper and lower limits of beam energy attenuation in the target are determined, formula (9) has clear evaluation significance.

## 1.2 Solid target design and target thickness calculation

### 1.2.1 Solid target design

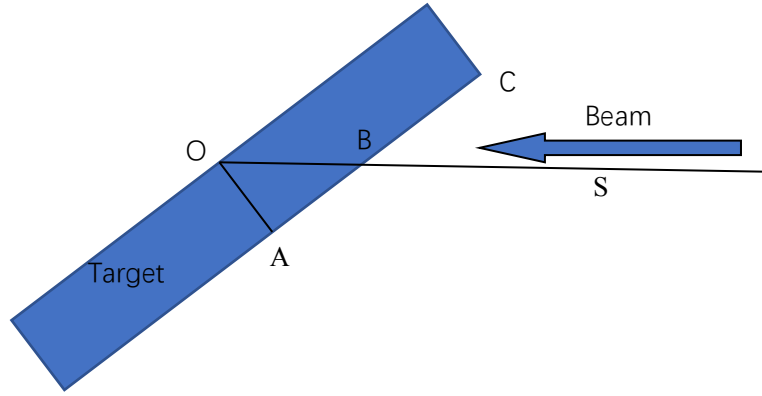


**Fig. 3 The diagram of Bombardment of solid target**

The solid target design is shown in Fig. 3. The beam bombards the tilted target from right to left, and it is assumed that the beam energy is completely deposited after the beam passes through the path BO in the target. The inclination Angle of the target is evaluated by the  $\angle SBC$  formed by the beam and the target plane ABC. According to the triangular relationship:  $\angle ABO = \angle SBC$ , so the corresponding target thickness  $AO = OB \cdot \sin \angle ABO$  when the beam penetration thickness is OB. When the beam injection energy is fixed, BO corresponds to the beam penetration depth is also fixed. Therefore, the more inclined the target and the smaller the thickness of the target is required to deposit all the energy.

### 1.2.2 Target thickness calculation

The energy lost after the inelastic collision between protons, alpha particles and extranuclear electrons through the unit path is the stopping power ( $-dE/dx$ ). When the charged particle beam deposits energy through the target, the ionization and excitation effects are the main forms of energy loss in formula (2), which is expressed in the Bethe-Block formula<sup>[25]</sup>:

$$\frac{1}{\rho} \left( \frac{dE}{dl} \right)_{col} = K_1 \frac{Z \cdot z^2}{M_A \beta^2} \left[ \ln \frac{(2\mu\beta)^2}{I^2(1-\beta^2)^2} - 2\beta^2 - 2\frac{C}{Z} - \delta \right] \dots\dots\dots (10)$$

$$K_1 = \frac{2\pi e^4 N_A}{mc^2} \dots\dots\dots (11)$$

In the formula:  $Z$  represents the atomic number of the target,  $z$  represents the number of charges carried by a single beam particle,  $m$  is the rest mass of the electron,  $c$  is the light speed,  $\beta = v/c$  is the relativistic velocity of the beam particle,  $v$  is the laboratory reference speed of the beam particle,

$\mu = mc^2$  is the rest energy of the electron (0.511MeV),  $M_A$  is the relative atomic or molar mass of the target,  $I$  is the average excitation energy of the atoms in the matter ( $I = I_0 Z = 10eV \cdot Z$ ),  $C/Z$  is the shell correction term,  $\delta$  is the density dependent correction term,  $N_A$  is the Avogadro constant. Formula (10) corresponds to formula (4).

In the electrochemical preparation of the target, different electroplating processes will electroplate the target of different density and different thickness, and the thickness of the coating needs to be calculated according to the actual situation. In practice, it is difficult to obtain the density and thickness of the target without destroy the target, so it is necessary to evaluate the thickness of the target according to theoretical methods.

In formula (10), the square brackets are dimensionless parameters, so put the expression of  $K_1$  into the Bethe-Block formula:

$$\frac{1}{\rho} \left( \frac{dE}{dl} \right)_{col} \propto \frac{2\pi e^4 \cdot N_A \cdot Z \cdot z^2}{m \cdot M_A \cdot v^2} \dots\dots\dots (12)$$

The relationship between kinetic energy and velocity of heavy charged particles at low velocity is

$$E = \frac{1}{2} m_p v^2, \quad m_p \text{ is the mass of the heavy charged particle, hence:}$$

$$dl \propto \frac{1}{\rho} \frac{m \cdot M_A \cdot v^2}{2\pi e^4 \cdot N_A \cdot Z \cdot z^2} dE \propto \frac{1}{\rho} \frac{m \cdot M_A \cdot v^3 \cdot m_p dv}{2\pi e^4 \cdot N_A \cdot Z \cdot z^2} \dots\dots\dots (13)$$

Thus the penetration depth is obtained:

$$R = \int_0^{R(E_0)} dl \propto \int_0^{v(E_0)} \frac{1}{\rho} \frac{m \cdot M_A \cdot v^3 \cdot m_p}{2\pi e^4 \cdot N_A \cdot Z \cdot z^2} dv \dots [cm] \dots\dots\dots (14)$$

$$R \propto \int_0^{v(E_0)} \frac{1}{\rho} \frac{M_A \cdot v^3 \cdot m_p}{Z \cdot z^2} dv \dots [cm] \dots\dots\dots (15)$$

It can be seen from formula (15) that the beam penetration depth is related to the density  $\rho$  of the prepared target, the atomic number  $Z$  of the target, the relative atomic mass  $M_A$  of the target, the charge number  $z$  carried by a single beam particle, the mass  $m_p$  of the beam particle, and the beam velocity  $v$  (beam energy  $E$ ). It is difficult to evaluate the thickness of the target with different densities due to

different electroplating processes. Formula (15) is transformed to obtain the mass thickness  $D$  of the electroplating target:

$$D = \rho R \propto \int_0^{v(E_0)} \frac{M_A \cdot v^3 \cdot m_p}{Z \cdot z^2} dv \dots [g \cdot cm^{-2}] \dots \quad (16)$$

It can be seen from formula (16) that the plating mass thickness of the target is not related to the plating density of the target, but is only related to the atomic number  $Z$  of the target, the relative atomic mass  $M_A$  of the target, the charge number  $z$  carried by a single beam particle, the beam particle mass  $m_p$ , and the beam velocity  $v$  (beam energy  $E$ ). In general, the mass thickness required for the beam to penetrate the target is only related to the target and beam parameters, and has nothing to do with the density of the target.

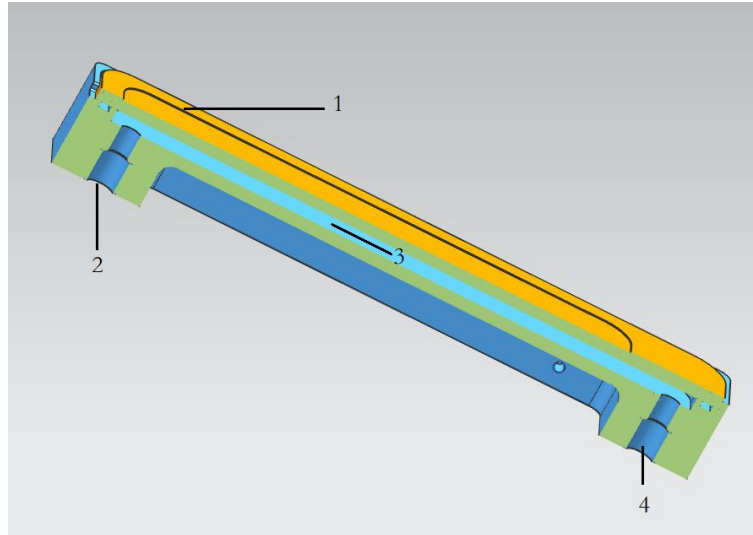


**Fig. 4 Design of the solid target: 1. Solid target plate; 2. Water cooling inlet; 3. Water cooling channel; 4. Water cooling outlet**

To reduce the amount of  $^{64}\text{Ni}$  used during irradiation, a tilt design of  $30^\circ$  is adopted during irradiation. The schematic diagram of the irradiation target is shown in Figure 4, and its compositions are: 1. Solid target plate; 2. Water cooling inlet; 3. Water cooling channel; 4. Water cooling outlet. The beam energy of the LB-11MTS is about 11MeV, and after passing through the vacuum window film, helium cooling chamber and target film, the beam energy entering the target is about 10.5MeV. The solid target  $^{64}\text{Ni}$  is designed with a tilt of  $30^\circ$  to calculate the required thickness of the  $^{64}\text{Ni}$  target.

In order to verify the above theory, the penetration depth of 10.5MeV proton was simulated by Monte Carlo program SRIM<sup>[26]</sup>, and the corresponding mass thickness was obtained.

### 1.3 Electroplating device design

The design of the electroplating device mainly refers to Faraday's law of electrolysis, Faraday's first law of electrolysis: in the electrochemical process, the mass of the substance reduced in the electric cathode is proportional to the amount of charge passed by the electrochemical circuit. The expression formula is as follows<sup>[27]</sup>:

$$m = KQ = KIt \dots\dots\dots (17)$$

Faraday's second law of electrolysis is: In an electrochemical reaction, the mass of the substance precipitated at the cathode is proportional to its electrochemical equivalent by the same total amount of charge.

$$K = \frac{M}{n \cdot F} \dots\dots\dots (18)$$

In the above two formulas,  $m$  represents the mass of the material precipitated by the electric cathode,  $Q = It$  represents the amount of charge equal to the accumulation of current to time,  $M$  represents the molar mass of the substance g/mol,  $n$  represents the valence of the substance in the electroplating solution,  $F$  is the Faraday constant, represents the amount of charge carried by 1 mol of charge  $F = 6.022 \times 10^{23} \times 1.602 \times 10^{-19} \approx 96500 [C / mol]$ .  $K$  is the electrochemical equivalent, representing the mass deposited by the unit charge in the cathode, in g/C. Conversion of Faraday's constant:  $96500 [C/mol] = 26.8 [A \cdot h / mol]$ , The electrochemical equivalent can be expressed as:

$$K = \frac{M}{n \cdot 26.8} [g/(A \cdot h)] \dots\dots\dots (19)$$

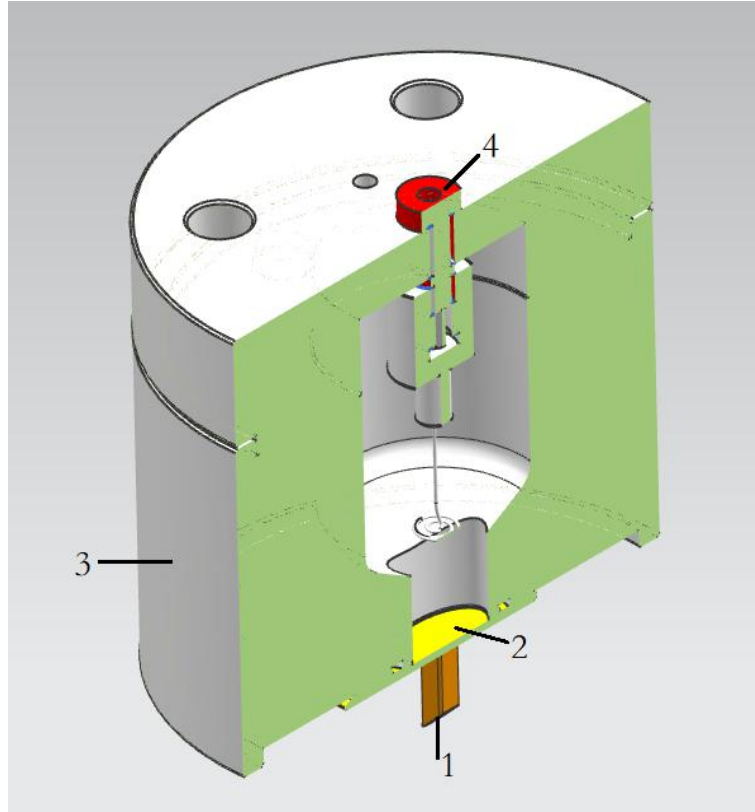


**Fig. 5 Diagram of the electroplating device: 1. Electric cathode; 2. Electroplating target film; 3. Main body of electroplating device; 4. Electric anode**

The design of  $^{64}\text{Ni}$  electroplating device based on electroplating principle is shown in Fig. 5, including 1. Electric cathode; 2. Electroplating target film; 3. Main body of electroplating device; 4. Electric anode. After the electroplating solution is loaded into the main body of the electroplating device, the anode and cathode of the device are loaded. The cation in the electroplating solution will move to the electroplating target under the action of electric field force, and the cation will obtain electrons on the electroplating target to form  $^{64}\text{Ni}$  atoms, and finally deposit on the target continuously.

In actual electroplating, the actual mass  $m_0$  of the precipitated material on the electro cathode is different from the theoretical calculation  $m$ , so the electroplating efficiency is defined:

$$\eta = \frac{m_0}{m} = \frac{m_0}{(KIT)} \times 100\% \dots\dots\dots (20)$$

According to the electrolytic law, electrochemical equivalent and current efficiency formula, the formula for the thickness of the coating can be derived as follows:

$$\delta = \frac{V}{S} = \frac{m_0}{S \cdot \rho_0} = \frac{I \cdot t \cdot K \cdot \eta}{S \cdot \rho_0} \dots\dots\dots (21)$$

In the above formula,  $V$  is the volume of the plating layer,  $S$  is the area of the plating area, and  $\rho_0$  is the density of the plating layer. However, in practice, the plating layer density is different due to different plating processes such as the plating solution concentration and electroplating current power supply mode. According to formula (16), in practice, we only need the mass thickness of the coating, so it can be used for irradiation only if the coating meets the irradiation conditions.

#### 1.4 Solid target electroplating process

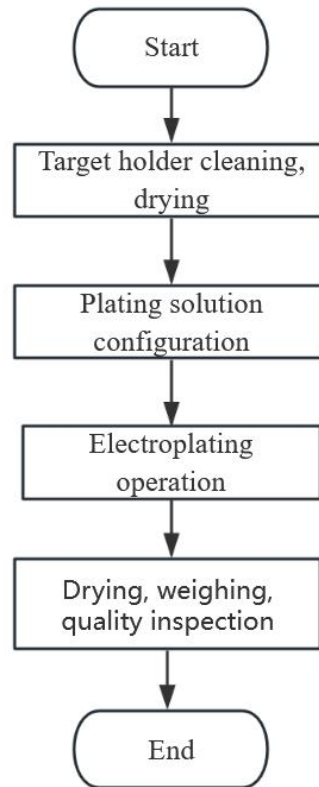
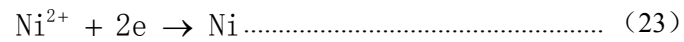
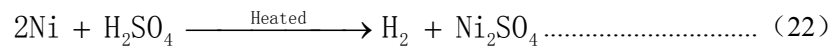


**Fig. 6 Target process of electroplating**

The solid target plating process is mainly shown in Fig. 6, which mainly includes target holder cleaning and drying, plating solution configuration, plating operation, completion of plating target drying, weighing and quality inspection. The main process of cleaning operation: degreasing operation with 0.1mol/L nitric acid, ultrasonic shock cleaning with pure water, etc. After cleaning, the target plate is dried and weighed, and the initial mass  $M_0$  of the target plate before electroplating is recorded. After electroplating, the target plate is dried and weighed again, the mass  $M_1$  of the target plate after electroplating is recorded, and the mass thickness  $D_i = (M_1 - M_0) / S$  of the target plate on the electroplating can be calculated according to the electroplating area  $S$ . According to formula (16),

whether the mass thickness of the electroplating target plate meets the requirements can be determined. The plating solution configuration mainly includes Ni material weighing, adding 18M sulfuric acid to Ni, heating dissolution and other processes. After dissolution, to match the electroplating environment, it is necessary to neutralize and dilute the solution with ammonia and pure water, and adjust the PH of the electroplating solution to 9.5-10. During the plating process, 20mA DC power supply is used for plating 15 hours.

The main chemical reaction formulas of Ni dissolution and electroplating process are shown in formula (22) and (23) respectively



## 2 Results and Analysis

### 2.1 Stopping power calculation results

According to the nuclear reaction probability ratio formula, the energy decay curve  $-dE/dx$  is needed, which is calculated by SRIM. According to formula (4), the energy decay curves obtained with different densities are different, and the stopping power curves of targets with different densities are as follows:

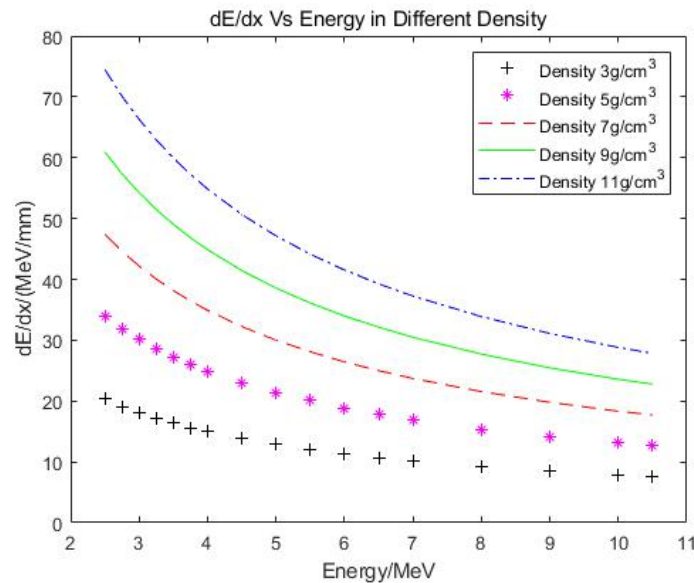


**Fig. 7 Relation between stopping power and beam energy of different density targets**

According to formula (4), the stopping power  $-dE/dx$  is proportional to the density of the target and inversely proportional to the energy of the beam. Therefore, the inverse energy ratio curve fitting was carried out on the simulated target of 9 g/cm³ and the fitting results were shown in Fig. 8 and formula (24):

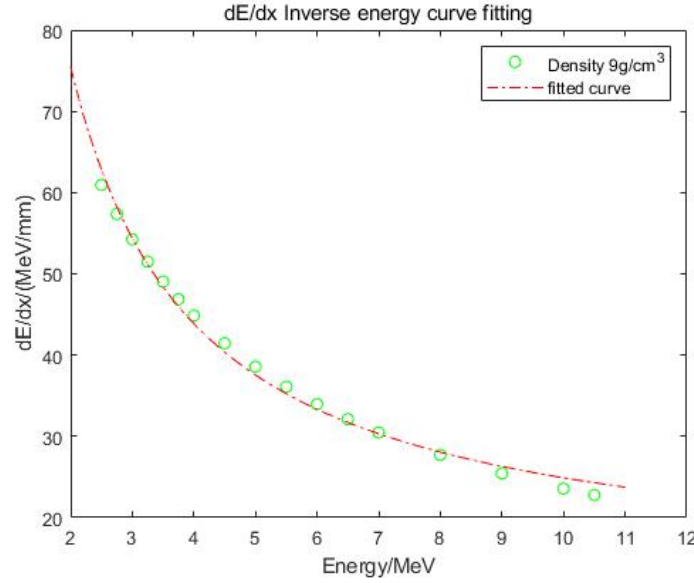


**Fig. 8 Inverse ratio of stopping power and energy is fitted**

$$\begin{cases} dE / dx = 126.5 / E + 12.25 \\ R^2 = 0.99353 \end{cases} \dots\dots\dots (24)$$

It can be seen from the fitting results of Fig. 8 and formula (22) that the simulation experiment results are consistent with the theoretical analysis, and the fitting results can be used to analyze the nuclear reactions probability ratio.

## 2.2 The nuclear reaction cross section ratio and the nuclear reaction probability ratio

In this paper, the  $^{64}\text{Ni}(p,n)^{64}\text{Cu}$  nuclear reaction was carried out by the LB-11MTS cyclotron to study the preparation technology of  $^{64}\text{Cu}$  radionuclide target. The LB-11MTS cyclotron can produce 11MeV proton beam and the max beam current is above 100 $\mu\text{A}$ . After the beam passing through the vacuum window film, helium cooling chamber and target film, the beam energy entering the target is about 10.5MeV. So, the maximum beam energy hitting the  $^{64}\text{Ni}$  target is calculated as 10.5MeV. According to formula (8), the proportion of nuclear reaction cross sections and the proportion of nuclear reaction probability of the beam outgoing beam target with the energy of 2.6MeV~7.5 MeV are calculated. The data of nuclear reaction cross sections are obtained from the IAEA official website [23]. The calculation of 4MeV energy exiting the target is shown in equation (25).

$$\eta_1 = \frac{\int_{10.5}^4 \sigma(E)dE}{\int_0^{10.5} \sigma(E)dE} \dots\dots\dots (25)$$

According to formula (9), the probability proportion of nuclear reactions ranging from 4MeV to 10.5MeV is calculated as follows:

$$\eta_2 = \frac{\int_4^{10.5} \frac{\sigma(E)}{-dE/dx} dE}{\int_0^{10.5} \frac{\sigma(E)}{-dE/dx} dE} \dots\dots\dots (26)$$

In the calculation, the stopping power  $-dE/dx$  is calculated by 9 g/cm<sup>3</sup> target material SRIM results.

Based on Formulas (25) and (26), when a 10.5 MeV proton beam is incident on the target surface and different energy beams exit the target, the proportion of nuclear reaction cross-sections and the proportion of nuclear reaction probabilities are shown in Table 1:

**Talbe.1 Results of the proportion of nuclear reaction cross section and the proportion of nuclear reaction probability**

Energy	Energy~10.5MeV Cross Section Integral	Cross Section Ratio	Energy~10.5MeV Probabilities Integral	Probabilities Ratio
MeV	mb*MeV			
2.60	2990.83	100.00%	8.87E-04	100.00%
3.00	2988.69	99.93%	8.86E-04	99.94%
3.50	2975.57	99.49%	8.84E-04	99.63%
4.00	2937.94	98.23%	8.76E-04	98.76%
4.50	2887.49	96.54%	8.65E-04	97.49%
5.00	2804.41	93.77%	8.45E-04	95.28%
5.50	2681.83	89.67%	8.15E-04	91.87%
6.00	2531.71	84.65%	7.72E-04	87.03%
6.50	2336.92	78.14%	7.23E-04	81.51%
7.00	2124.06	71.02%	6.63E-04	74.73%
7.50	1882.45	62.94%	5.92E-04	66.77%

According to the calculation results, it can be known that because the stopping power  $-dE/dx$  of the material to the beam is added to the proportion of the nuclear reaction probability, the result of the proportion of the nuclear reaction probability is slightly larger than that of the cross-section proportion. Since the formula of the proportion of the nuclear reaction probability is deduced from the yield of the nuclear reaction, therefore, the result of the proportion of the nuclear reaction probability is of more reference significance for the thickness design of the expensive target material. Based on the calculation results of the cross-section proportion and the proportion of the nuclear reaction probability, the energy of the beam emitted from the target material is selected to be 5.5 MeV.

### 2.3 The yield calculation

It can be known from Table 1 that when a proton beam with an energy of 10.5 MeV is incident on the <sup>64</sup>Ni target and exits at 5.5 MeV, the nuclear reaction probability integral is: 8.15E - 04. Thus, information

such as the saturation yield can be obtained. The yield information of the incident energy of 10.5 MeV and the exit energy of 2.6 MeV is compared as shown in the following table:

**Talbe.2 The yield results of 10.5MeV proton incident on the target with energies of 2.5MeV and 5.5MeV proton exiting the target**

Exiting Target Energy MeV	Saturation Yield MBq/μA	Saturation Yield mCi/μA	1h Yield mCi/μA/h
5.50	5.09E+03	137.48	7.30
2.60	5.53E+03	149.57	7.94

It can be known from the results in Table 2 that when the incident proton beam with an energy of 10.5 MeV exits the target material at 5.5 MeV, the yield is approximately 7.3 mCi/μA/h, accounting for 91.94% of the target material exiting at 2.6 MeV. Therefore, in terms of theoretical yield calculation, it is feasible and effective to evaluate and select the nuclear reaction energy range through the proportion of nuclear reaction cross-section and the proportion of nuclear reaction probability.

#### 2.4 The calculation results of target thickness

When the beam penetrates the target material, the energy attenuation curve along the unit path can be calculated by referring to the stopping power formula. It is demonstrated in the previous text that the stopping power  $-dE/dx$  is proportional to the density  $\rho$  of the target material and inversely proportional to the beam energy. In actual electroplating, different electroplating target-making processes will result in target materials with different densities. Referring to Formula (16) and using the SRIM Monte Carlo program, when calculating the 10.5 MeV proton beam incident on  $^{64}\text{Ni}$  target materials with different densities, the parameters of the required target material thickness and mass thickness when the beam exits the target material with different energies are shown in Table 3. In Table 3, according to the irradiation scheme design in Fig. 3 and Fig. 4, the parameters of the required target thickness and mass thickness when the beam is incident perpendicularly to the target and at an angle of  $30^\circ$  to the target sheet are also obtained.

**Talbe.3 The target thickness and surface density parameters of the 0、2.6 and 5.5MeV proton emission targets were obtained when 10.5MeV proton incident on targets with different densities**

Densities	0MeV Depths	0MeV, $30^\circ$ Depths	0MeV, $30^\circ$ Mass Thickness	2.6MeV Depths	2.6MeV, $30^\circ$ Depths	2.6MeV, $30^\circ$ Mass Thickness
g/cm <sup>3</sup>	μm	um	mg/cm <sup>2</sup>	um	um	mg/cm <sup>2</sup>
3	816	408	122.4	732	366	109.8
5	489	244.5	122.25	441	220.5	110.25

7	349	174.5	122.15	315	157.5	110.25
9	272	136	122.4	245	122.5	110.25
11	222	111	122.1	201	100.5	110.55
密度	4MeV Depths	4MeV, 30° Depths	4MeV, 30° Mass Thickness	5.5MeV Depths	5.5MeV, 30° Depths	5.5MeV, 30° Mass Thickness
g/cm <sup>3</sup>	um	um	mg/cm <sup>2</sup>	um	um	mg/cm <sup>2</sup>
3	652	326	97.8	540	270	81.00
5	391	195.5	97.75	324	162	81.00
7	279.4	139.7	97.79	230	115	80.50
9	217.4	108.7	97.83	180	90	81.00
11	177.5	88.75	97.625	147	74	80.85
密度	6.5MeV Depths	6.5MeV, 30° Depths	6.5MeV, 30° Mass Thickness	7.5MeV Depths	7.5MeV, 30° Depths	7.5MeV, 30° Mass Thickness
g/cm <sup>3</sup>	um	um	mg/cm <sup>2</sup>	um	um	mg/cm <sup>2</sup>
3	450	225	67.5	350	175	52.5
5	270	135	67.5	211	105.5	52.75
7	194	97	67.9	150	75	52.5
9	151	75.5	67.95	117	58.5	52.65
11	123	61.5	67.65	95.6	47.8	52.58

In Table 3, "depth" corresponds to the thickness of the target material. When the energy of the beam incident on the target and the energy emitted from the target are constant, the greater the density of the electroplated target, the smaller the thickness of the required target, but the mass thickness is basically constant. Therefore, in the electroplating design, the mass thickness parameter of the target is used as the main quality control parameter for electroplating target fabrication. In the case of 30° beam irradiation of the target, and proton energies of 0, 2.6, 4, 5.5, 6.5, and 7.5 MeV for the emitted target, the required target mass thicknesses are approximately: 122, 110, 98, 81, 68, and 53 mg/cm<sup>2</sup>, respectively.

Referring to the above text, when the energy of the proton emitted from the target material is selected as 5.5 MeV, the yield efficiency is 91.94% of that of the 0 MeV and 2.6 MeV beam emitted from the target material, and the required target material masses correspond to 66.39% and 73.64% respectively.

## 2.5 The electroplating equipment and electroplating process



**Fig. 9 Electroplating equipment**

The equipment used in the electroplating process is shown in the figure. It is the IsotopeX Lab series TPS 1.0 electroplating device independently developed by Sichuan Longevous BeamTech Co., LTD, which can be used for the electroplating of various metal target sheets. According to the target sheet area of approximately  $1.815 \text{ cm}^2$ , and the incident of 10.5 MeV proton beam on the target sheet, and the required mass thickness of  $81 \text{ mg/cm}^2$  for the 5.5 MeV energy outgoing target sheet, the actual required amount of  $^{64}\text{Ni}$  can be calculated to be approximately 147 mg. According to the formula (18)  $K = M / (n \cdot F)$ , the electrochemical equivalent of Ni can be calculated to be  $0.33161 \text{ mg/C}$ . Therefore, according to the Faraday's first law of electrolysis formula (17)  $m = KQ = KIt$ , the total required charge can be calculated to be 443.29 C. If a 20 mA DC power supply is used, the required electroplating time is approximately 6.2 hours. Actually, based on methods such as process debugging, using a 20 mA DC power supply for 12 hours of electroplating, the electroplating results are shown in Figure 10: For different applications, the left side is the designed elliptical  $^{64}\text{Ni}$  target, and the right side is the designed circular  $^{64}\text{Ni}$  target.

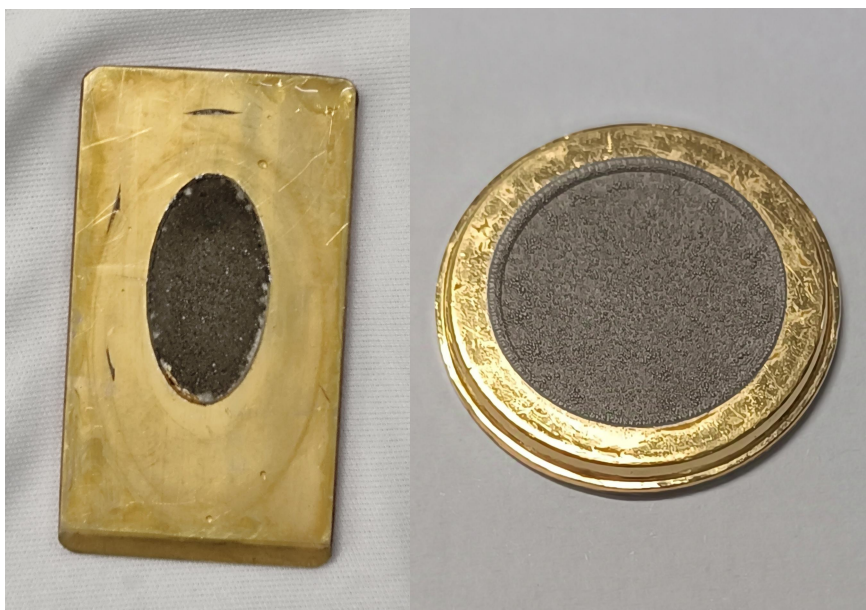


**Fig. 10** The left side of the electroplating target is elliptical, the right side is circular

## 2.7 Irradiation

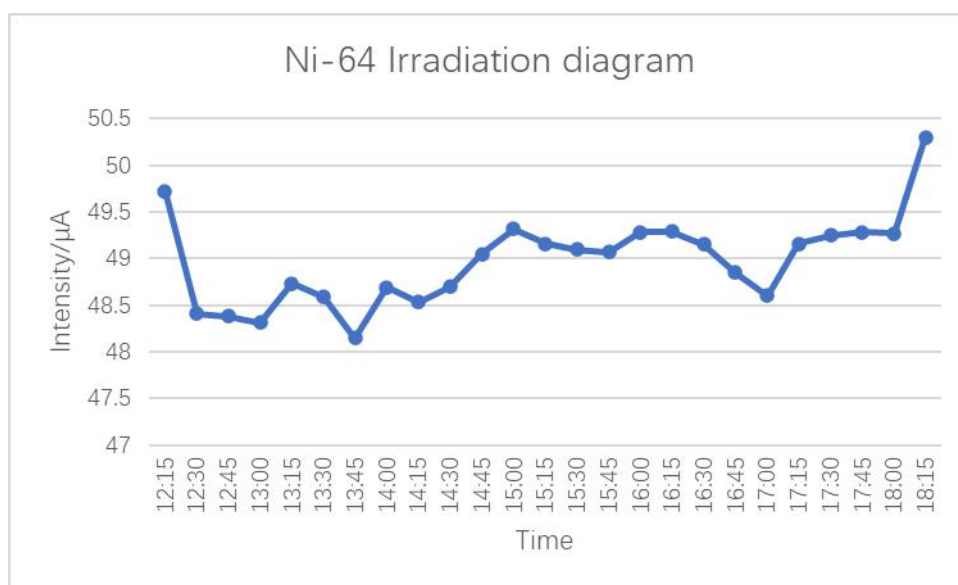


**Fig. 11** The time diagram of Nickel-64 target irradiated

The electroplated target sheet was irradiated and bombarded using cyclotron proton beam. The bombardment time is shown above. The average beam current on the target was approximately 48.97  $\mu\text{A}$ , and the irradiation time was 6 hours, obtaining  $^{64}\text{Cu}$  radioactive activity of 1.34 Ci. According to the above discussion, the theoretical yield was:  $7.3 * 48.97 * 6 = 2.14$  Ci. The reason for the low yield was that the mass thickness of this target sheet was  $58.6 \text{ mg/cm}^2$ , which was relatively lower than the required value of  $81 \text{ mg/cm}^2$ . Comparing Table 3, it can be estimated that the energy of the proton beam exiting the target material was approximately 7 MeV. Combining with Table 2, the yield was approximately 74.73% of the total energy deposition. Therefore, for the 7 MeV beam exiting the target material, the yield was approximately: 1.74 Ci. The radioactive activity was monitored, and the results are shown in Fig. 12. In Fig.

12 the decay constant obtained by fitting was 0.05731/h, which was converted to a half-life of 12.09 hours, which was basically consistent with the half-life of  $^{64}\text{Cu}$ . The gamma energy spectrum test was performed on the target sheet after the bombardment, and the test results are shown in Figure 13. The gamma energy spectrum results show that there was a sharp peak on the Compton scattering platform. The possible reason was that the target sheet contained other radionuclides immediately after the bombardment.

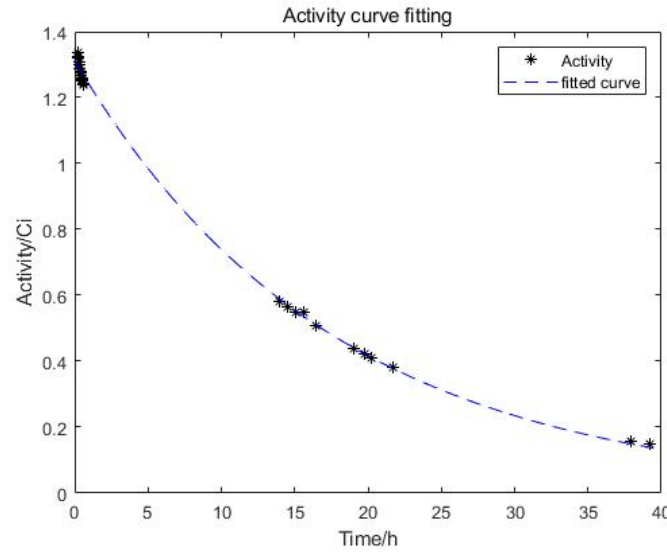


**Fig. 12 The Activity diagram of Copper-64**

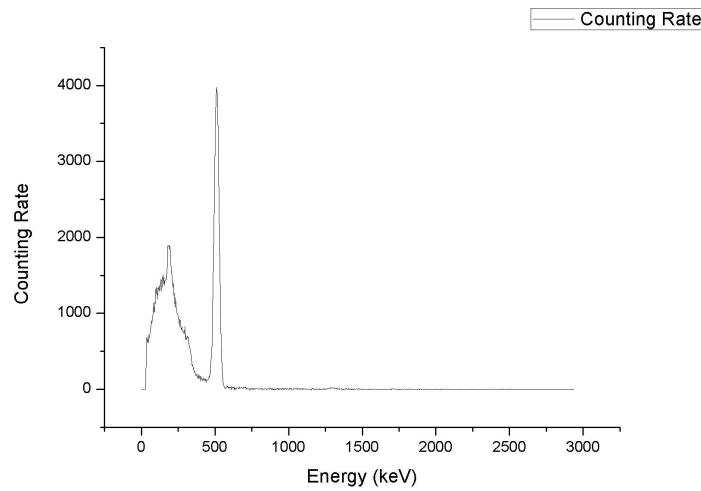


**Fig. 13 The Gamma spectrum of Copper-64**

### 3 Discussion

For elemental targets, referring to formulas (2), (3), and (4), the probability of nuclear reaction occurring when a beam of a certain energy is incident on the target is related to the upper and lower limits of the deposited energy of the beam, the charge number  $z$  of the charged beam, the atomic number  $Z$  of the target. It is not related to the atomic density  $N_v$  of the target, and the relative atomic mass  $M_A$ , and

the density  $\rho$  of the target. For nuclides such as  $^{124}\text{I}$  and  $^{44}\text{Sc}$ , the target needs to be powder-pressed and sintered, and the target is a compound or a mixture of multiple compounds. If the average excitation energy of atoms remains unchanged, for compound or mixture targets, the formula for the probability of nuclear reaction between the beam and the target is as follows:

$$\left\{ \begin{array}{l} P = N_v \int_0^{E_0} \left[ \frac{\sigma(E)}{-dE/dx} \right] \cdot dE = \frac{\rho_i \cdot N_A}{M_A} \int_0^{E_0} \left[ \frac{\sigma(E)}{-dE/dx} \right] \cdot dE \\ -\frac{dE}{dx} = \frac{4\pi z^2 e^4 Z_{eff} \rho_i N_A}{m(v^2 M_A)} \left[ \ln\left(\frac{2mv^2}{I}\right) - \ln(1 - \beta^2) - \beta^2 \right] \\ Z_{eff}^n = \sum C_i \cdot Z_i^n \\ \rho_i = \frac{m_i}{V} = \frac{m_i}{\sum m_i} \cdot \frac{\sum m_i}{V} = C_i \cdot \rho \\ N_v = \frac{N}{V} = \frac{\frac{m_i}{M_A} \cdot N_A}{V} = \rho_i \cdot \frac{N_A}{M_A} \\ \rho = \sum m_i / V = \sum \rho_i \end{array} \right. \dots\dots\dots (27)$$

In Formula (27),  $C_i$  represents the element content of a certain element in the entire target material,  $Z_{eff}$  represents the effective atomic number of the compound or mixture target material<sup>[28]</sup>, and  $\rho_i$  represents the element density of a certain element in the target material. The nuclear reaction probability of the beam with the compound or mixture target material are related to the upper and lower energy limits of the beam, and the charge number  $z$  of the charged beam, the effective atomic number  $Z_{eff}$  of the target material, and are positively correlated with the element content  $\sqrt[n]{C_i}$ . The specific value of  $n$  is related to the type of the acting beam current.

The main factors affecting the radionuclide purity and radiochemical purity include the purity of the target material, the energy related to the incident and exit of the beam on the target material, and the subsequent chemical purification process. To produce  $^{64}\text{Cu}$  by using  $^{64}\text{Ni}$  target material, the  $^{64}\text{Ni}(p,2n)^{63}\text{Cu}$  reaction will occur when the beam energy is greater than 11 MeV, and  $^{63}\text{Cu}$  is a stable nuclide. When the proton beam energy is 17 MeV, the nuclear reaction cross section for the production of  $^{63}\text{Cu}$  is 768.75 mb, which is comparable to that for the production of  $^{64}\text{Cu}$ .  $^{64}\text{Cu}$  and  $^{63}\text{Cu}$  are difficult to be separated by chemical purification. If the incident beam energy is too high, the prepared Cu nuclides will affect the radiochemical purity and labeling efficiency of the drug.

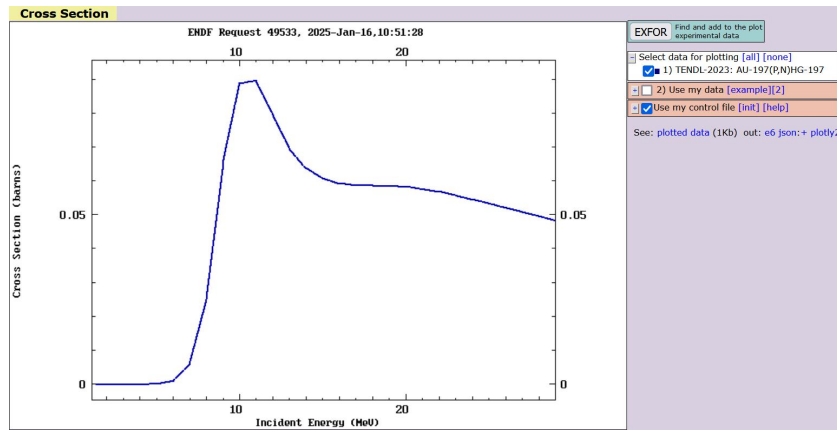


**Fig. 14 The nuclear reaction of  $^{197}\text{Au}(\text{p},\text{n})^{197}\text{Hg}$**

After the beam is emitted and hits the target material, the outgoing beam will deposit the remaining energy on the target holder. If the energy hitting the target holder is higher than the threshold energy of the nuclear reaction between the beam and the target holder, it will cause radioactive contamination of the target holder. In the preparation of the  $^{64}\text{Cu}$  isotope, a gold target holder is used. Querying the EXFOR data reveals that when protons with an energy greater than 3.13 MeV are incident on the gold target holder, the  $^{197}\text{Au}(\text{p},\text{n})^{197}\text{Hg}$  nuclear reaction occurs as shown in Fig. 14, and this reaction will cause the radioactive contamination problem of the target holder.  $^{197}\text{Hg}$  undergoes EC decay with a half-life of 64.14 hours. The assessment of the radioactive nuclear reaction of the target holder can be studied by referring to the methods of the proportion of nuclear reaction cross-sections and the proportion of nuclear reaction probabilities in this article.

## 4 Conclusion

This paper systematically discussed the nuclear reaction principle of proton beam and  $^{64}\text{Ni}$  target material, and theoretically demonstrated the mass thickness parameters of  $^{64}\text{Ni}$  target sheet, and the stopping power was calculated. For the expensive target material, the methods of nuclear reaction cross-section ratio and nuclear reaction probability ratio were proposed for evaluation. The conclusion was drawn that when a 10.5 MeV proton beam is incident on the target material and a 5.5 MeV proton beam is emitted from the target material, the cost of the target material is 66.39% of the total energy deposition, but the yield is 91.94% of the total energy deposition. Moreover, an electroplating device was designed based on the electroplating principle, and finally  $^{64}\text{Ni}$  target sheets were electroplated. The target was bombarded with an average current intensity of 48.97  $\mu\text{A}$  for 6 hours, and the radioactive activity of  $^{64}\text{Cu}$  obtained was 1.338 Ci.

## References :

- [1] Boschi A, Martini P, Janevik-Ivanovska E, et al. The emerging role of copper-64 radiopharmaceuticals as cancer theranostics[J]. *Drug Discovery Today*, 2018, 23(8): 1489-1501.
- [2] REPO A L S, TS N. Cyclotron Produced Radionuclides: Emerging Positron Emitters for Medical Applications:  $^{64}\text{Cu}$  and  $^{124}\text{I}$ [J].
- [3] Alves F, Alves V H P, Do Carmo S J C, et al. Production of copper-64 and gallium-68 with a medical cyclotron using liquid targets[J]. *Modern Physics Letters A*, 2017, 32(17): 1740013.
- [4] Evangelista L, Luigi M, Lucio Cascini G. New issues for copper-64: from precursor to innovative PET tracers in clinical oncology[J]. *Current Radiopharmaceuticals*, 2013, 6(3): 117-123.
- [5] Panichelli P, Villano C, Cistaro A, et al. Imaging of brain tumors with copper-64 chloride: early experience and results[J]. *Cancer Biotherapy and Radiopharmaceuticals*, 2016, 31(5): 159-167.
- [6] Kjærgaard K, Sandahl T D, Frisch K, et al. Intravenous and oral copper kinetics, biodistribution and dosimetry in healthy humans studied by [ $^{64}\text{Cu}$ ] copper PET/CT[J]. *EJNMMI Radiopharmacy and Chemistry*, 2020, 5: 1-12.
- [7] Capriotti G, Piccardo A, Giovannelli E, et al. Targeting copper in cancer imaging and therapy: a new theragnostic agent[J]. *Journal of Clinical Medicine*, 2022, 12(1): 223.
- [8] Pretze M, van der Meulen N P, Wängler C, et al. Targeted  $^{64}\text{Cu}$  - labeled gold nanoparticles for dual imaging with positron emission tomography and optical imaging[J]. *Journal of Labelled Compounds and Radiopharmaceuticals*, 2019, 62(8): 471-482.
- [9] Singh G, Zarschler K, Hunoldt S, et al. Versatile Bispidine - Based Bifunctional Chelators for  $^{64}\text{CuII}$  - Labelling of Biomolecules[J]. *Chemistry—A European Journal*, 2020, 26(9): 1989-2001.
- [10] McMahon J H, Zerbato J M, Lau J S Y, et al. A clinical trial of non-invasive imaging with an anti-HIV antibody labelled with copper-64 in people living with HIV and uninfected controls[J]. *EBioMedicine*, 2021, 65.
- [11] Earley D F, Flores J E, Guillou A, et al. Photoactivatable bis (thiosemicarbazone) derivatives for copper-64 radiotracer synthesis[J]. *Dalton Transactions*, 2022, 51(13): 5041-5052.
- [12] Krasnovskaya O O, Abramchuck D, Erofeev A, et al. Recent advances in  $^{64}\text{Cu}/^{67}\text{Cu}$ -based radiopharmaceuticals[J]. *International Journal of Molecular Sciences*, 2023, 24(11): 9154.
- [13] 许国基,孟祥金,罗兴华等.核靶厚度和均匀性测量[J].*原子能科学技术*,1991,25(3):34-39.  
Xu Guoji, Meng Xiangjin, Luo Xinghua et al. Measurement of thickness and uniformity of nuclear target [J]. *Atomic Energy Science and Technology*,1991,25(3):34-39. (in Chinese)
- [14] 许国基,关守仁,罗兴华等.同位素靶制备技术的研究[J].*原子能科学技术*,1995,29(1):68-74.

- XU Guoji, Guan Shouren, Luo Xinghua et al. Study on preparation technology of isotope target [J]. Atomic Energy Science and Technology, 1995, 29(1): 68-74. (in Chinese)
- [15] McCarthy D W, Shefer R E, Klinkowstein R E, et al. Efficient production of high specific activity  $^{64}\text{Cu}$  using a biomedical cyclotron[J]. Nuclear medicine and biology, 1997, 24(1): 35-43.
- [16] Obata A, Kasamatsu S, McCarthy D W, et al. Production of therapeutic quantities of  $^{64}\text{Cu}$  using a 12 MeV cyclotron[J]. Nuclear medicine and biology, 2003, 30(5): 535-539.
- [17] Kim J Y, Park H, Lee J C, et al. A simple Cu-64 production and its application of Cu-64 ATSM[J]. Applied Radiation and Isotopes, 2009, 67(7-8): 1190-1194.
- [18] 孙夕林, 王凯, 林艳红, 等. 医用回旋加速器的  $^{64}\text{Cu}$  高效制备[J]. Progress in Modern Biomedicine, 2016, 16(19).
- Sun Xilin, Wang Kai, Lin Yan-Hong, et al. Efficient preparation of  $^{64}\text{Cu}$  by medical cyclotron [J]. Progress in Modern Biomedicine, 2016, 16(19). (in Chinese)
- [19] Xie Q, Zhu H, Wang F, et al. Establishing reliable Cu-64 production process: from target plating to molecular specific tumor micro-PET imaging[J]. Molecules, 2017, 22(4): 641.
- [20] Jauregui-Osoro M, De Robertis S, Halsted P, et al. Production of copper-64 using a hospital cyclotron: targetry, purification and quality analysis[J]. Nuclear Medicine Communications, 2021, 42(9): 1024-1038.
- [21] Hrynchak I, Cocioabă D, Fonseca A I, et al. Antibody and Nanobody Radiolabeling with Copper-64: Solid vs. Liquid Target Approach[J]. Molecules, 2023, 28(12): 4670.
- [22] INTERNATIONAL ATOMIC ENERGY AGENCY, Cyclotron Produced Radionuclides: Physical Characteristics and Production Methods, Technical Report Series No. 468, IAEA, Vienna, (2009)
- [23] <https://www-nds.iaea.org/medical/nip64cu0.html>
- [24] 卢希庭主编.原子核物理 修订版[M].北京: 原子能出版社,2000.
- Lu Xiting (Ed.). Nuclear Physics Revision [M]. Beijing: Atomic Energy Press, 2000. (in Chinese)
- [25] 祥云, 刘元方.核化学与放射化学[M].北京大学出版社,2007.
- Xiang Yun, Liu Yuanfang. Nuclear Chemistry and Radiochemistry [M]. Peking University Press, 2007. (in Chinese)
- [26] <http://www.srim.org/>
- [27] 徐致远, 戴洁琼, 吴波等. 法拉第电解定律表述的辨析[J]. 凯里学院学报, 2015, 33(3): 175-176.
- Xu Zhiyuan, Dai Jieqiong, Wu Bo et al. Analysis of Faraday's Law of Electrolysis [J]. Journal of Kaili College, 2015, 33(3): 175-176.
- [28] 张伟军. 化合物或混合物的有效原子序数研究[J]. 核电子学与探测技术, 2013, 33(1): 120-126.

Zhang Weijun. Study on effective atomic number of Compounds or mixtures [J]. Nuclear Electronics and Detection Technology, 2013, 33(1): 120-126. (in Chinese)